arXiv:hep-ph/0410146v2 8 Dec 2004

Rare radiative leptonic decays $B_{d,s} \to \ell^+\ell^-\gamma$

Dmitri Melikhov and Nikolai Nikitin
Institute of Nuclear Physics, Moscow State University, 119992, Moscow, Russia

(Dated: February 2, 2008)

Long-distance QCD effects in $B_{d,s} \to \ell^+\ell^-\gamma$ decays are analyzed. We show that the contribution of the light vector-meson resonances related to the virtual photon emission from valence quarks of the B-meson, which was not considered in previous analyses, strongly influences the dilepton differential distrubution. Taking into account photon emission from the b-quark loop, weak annihilation, and Bremsstrahlung from leptons in the final state, we give predictions for dilepton spectrum in $B_{d,s} \to \ell^+\ell^-\gamma$ decays within the Standard Model.

PACS numbers: 13.20.He,12.39.Ki,12.39.Pn

I. INTRODUCTION

Rare radiative leptonic $B_{d,s} \to \ell^+\ell^-\gamma$ decays are induced by the flavour-changing neutral current transitions $b \to s, d$. In the Standard Model such processes are described by penguin and box diagrams and have small probabilities $10^{-8} - 10^{-15}$ (see e.g. [1]). Processes with such small branching ratios cannot be observed at the running machines such as Tevatron, BaBar and Belle. The decays $B_{d,s} \to \mu^+\mu^-$ and $B_{d,s} \to \mu^+\mu^-\gamma$ will be studied at LHC with the detectors ATLAS, CMS, and LHCb [2]. These decays are perspective candidates for a search for physics beyond the Standard Model, therefore reliable theoretical predictions for these decays are of great interest.

The effective Hamiltonian describing the $b \to q$ $(q = d, s)$ weak transition has the form [3]

$$\mathcal{H}_{\rm eff}^{b\to q} = \frac{G_F}{\sqrt{2}} V_{tb} V^*_{tq} \sum_i C_i(\mu)\, O_i(\mu), \qquad (1.1)$$

G_F being the Fermi constant, C_i the scale-dependent Wilson coefficients, and O_i the basis operators. For B decays $\mu \simeq 5$ GeV is a convenient choice. The amplitudes of the basis operators between the initial and final states may be parametrised in terms of the Lorentz-invariant form factors. For radiative leptonic decays several different basis operators contribute, and respectively, one encounters several different types of form factors. The latter contain nonperturbative QCD contributions, and therefore their calculation poses one of the main problems for theoretical analysis of $B \to \ell^+\ell^-\gamma$ decays.

The $B \to \ell^+\ell^-\gamma$ decays have been studied in several papers [4, 5, 6, 7, 8] where transition form factors have been analysed and partial widths, photon energy spectra, dilepton mass spectra, and charge asymetries have been calculated. It turns out however that an important contribution related to hadron resonance in the $\ell^+\ell^-$ channel was not taken properly into account. Our goal is to account for this contribution and to give reliable predictions for dilepton mass spectrum and decay rates.[1]

The paper is organized as follows: In Section II A we discuss the dominant contribution to the decay amplitude related to the transition $\langle\gamma|H_{\rm eff}(b \to q\ell^+\ell^-)|B\rangle$. In Section II B we study the contribution related to the $B \to \ell^+\ell^-$ transition induced by the photon penguin operator $\langle\ell^+\ell^-|\bar d\sigma_{\mu\nu}q|B\rangle$. For a proper description of this process it is necessary to take into account light meson resonances which emerge in the physical decay region. Making use of the vector meson dominance we relate these contributions to the $B \to V\gamma$ transition form factors. Weak annihilation is discussed in Section II C. This process is known to be suppressed by $1/m_b$ compared to the photon emission from the B-meson loop. Nevertheless, it gives sizeable contribution to the dilepton mass spectrum in the region of small dilepton momenta. In Section II D we consider Bremsstrahlung from leptons in the final state. Its contribution to the cross section is proportional to $(m_\ell/M_B)^2$ and is thus essentail mainly for τ leptons in the final state. In Section III we give numerical predictions for the branching ratios and dilepton mass spectra based on our detailed analysis of the form factors.

---

[1] We do not consider any asymmetries since they cannot be studied at LHC because of a small expected number of events [2].

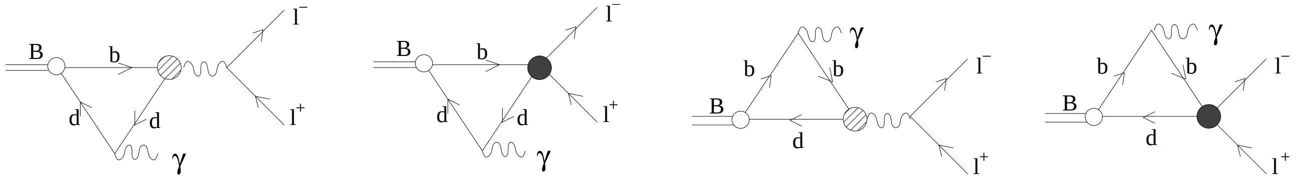

Fig. 1: Diagrams contributing to $B_d \to \ell^+\ell^-\gamma$ discussed in section II A. Dashed circles denote the $b \to d\gamma$ operator $O_{7\gamma}$. Solid circles denote the $b \to d\ell^+\ell^-$ operators O_{9V} and O_{10AV}.

II. THE $B \to \ell^+\ell^-\gamma$ AMPLITUDE

A. Direct emission of the real photon from valence quarks of the B meson

The amplitude of the process when real photon is directly emitted from the valence b or d quarks, and the $\ell^+\ell^-$ pair is coupled to the penguin is described by diagrams of Fig. 1. This amplitude is equal to $\langle\gamma|H_{\rm eff}^{b\to d\ell^+\ell^-}|B\rangle$ with[2]

$$\begin{aligned} H_{\rm eff}^{b\to d\ell^+\ell^-} &= \frac{G_F}{\sqrt{2}}\,\frac{\alpha_{\rm em}}{2\pi}\,V_{tb}V^*_{tq}\left[-2im_b\,\frac{C_{7\gamma}(\mu)}{q^2}\cdot\bar{d}\sigma_{\mu\nu}q^\nu\,(1+\gamma_5)\,b\cdot\bar{\ell}\gamma^\mu\ell\right.\\ &\left.\quad + C_{9V}^{\rm eff}(\mu,q^2)\cdot\bar{d}\gamma_\mu\,(1\,-\,\gamma_5)\,b\cdot\bar{\ell}\gamma^\mu\ell\,+\,C_{10A}(\mu)\cdot\bar{d}\gamma_\mu\,(1\,-\,\gamma_5)\,b\cdot\bar{\ell}\gamma^\mu\gamma_5\ell\right]. \end{aligned} \tag{2.1}$$

The coefficient $C_{9V}^{\rm eff}(\mu,q^2)$ includes long-distance effects related to $\bar{c}c$ resonances in the q^2-channel, q the momentum of the $\ell^+\ell^-$ pair [9]. The $C_{7\gamma}$ part in Eq. (2.1) emerges from the diagrams in Fig. 1 with the virtual photon emitted from the penguin

$$H_{\rm eff}^{b\to d\gamma} = \frac{G_F}{\sqrt{2}}\,V_{tb}V^*_{tq}\,C_{7\gamma}(\mu)\,\frac{e}{8\pi^2}\,m_b\cdot\bar{d}\,\sigma_{\mu\nu}\,(1+\gamma_5)\,b\cdot F^{\mu\nu}. \tag{2.2}$$

The $B \to \gamma$ transition form factors of the basis operators in (2.1) are defined according to [4]

$$\begin{aligned} \langle\gamma(k,\,\epsilon)|\bar{d}\gamma_\mu\gamma_5 b|B(p)\rangle &= i\,e\,\epsilon^*_\alpha\,(g_{\mu\alpha}\,pk - p_\alpha k_\mu)\,\frac{F_A(q^2)}{M_B},\\ \langle\gamma(k,\,\epsilon)|\bar{d}\gamma_\mu b|B(p)\rangle &= e\,\epsilon^*_\alpha\,\epsilon_{\mu\alpha\xi\eta}p_\xi k_\eta\,\frac{F_V(q^2)}{M_B},\\ \langle\gamma(k,\,\epsilon)|\bar{d}\sigma_{\mu\nu}\gamma_5 b|B(p)\rangle\,(p-k)^\nu &= e\,\epsilon^*_\alpha\,[g_{\mu\alpha}\,pk - p_\alpha k_\mu]\;F_{TA}(q^2,0),\\ \langle\gamma(k,\,\epsilon)|\bar{d}\sigma_{\mu\nu}b|B(p)\rangle\,(p-k)^\nu &= i\,e\,\epsilon^*_\alpha\epsilon_{\mu\alpha\xi\eta}p_\xi k_\eta\,F_{TV}(q^2,0). \end{aligned} \tag{2.3}$$

We treat the penguin form factors $F_{TV,TA}(q_1^2,q_2^2)$ as functions of two variables: q_1 is the momentum of the photon emitted from the penguin, and q_2 is the momentum of the photon emitted from the valence quark of the B meson. Usually one denotes $F_{TV,TA}(q^2,0) \equiv F_{TV,TA}(q^2)$. The form factors $F_{A,V,TA,TV}(q^2,0)$ were studied in detail in [4]. The parametrizations for these form factors from [4] which satisfy all known constraints in the limit $m_b \to \infty$ [10, 11] will be used in our analysis.

The amplitude corresponding to diagrams of Fig 1 takes the form [4]:

$$\begin{aligned} A^{(1)}_\mu &= \langle\gamma(k,\,\epsilon),\,\ell^+(p_1),\,\ell^-(p_2)\left|H_{\rm eff}^{b\to d\ell^+\ell^-}\right|B(p)\rangle = \frac{G_F}{\sqrt{2}}\,V_{tb}V^*_{tq}\,\frac{\alpha_{\rm em}}{2\pi}\,e\,\epsilon^*_\alpha\\ &\times\left[\frac{2\,C_{7\gamma}(\mu)}{q^2}\,m_b\,\left(\varepsilon_{\mu\alpha\xi\eta}p_\xi k_\eta\,F_{TV}(q^2,0)\,-\,i\,(g_{\mu\alpha}\,pk\,-\,p_\alpha k_\mu)\;F_{TA}(q^2,0)\right)\,\bar{\ell}(p_2)\gamma_\mu\ell(-p_1)\right.\\ &\quad C_{9V}^{\rm eff}(\mu,q^2)\left(\varepsilon_{\mu\alpha\xi\eta}p_\xi k_\eta\,\frac{F_V(q^2)}{M_B}\,-\,i\,(g_{\mu\alpha}\,pk\,-\,p_\alpha k_\mu)\,\frac{F_A(q^2)}{M_B}\right)\,\bar{\ell}(p_2)\gamma_\mu\ell(-p_1)\,+\\ &\quad\left.C_{10A}(\mu)\left(\varepsilon_{\mu\alpha\xi\eta}p_\xi k_\eta\,\frac{F_V(q^2)}{M_B}\,-\,i\,(g_{\mu\alpha}\,pk\,-\,p_\alpha k_\mu)\,\frac{F_A(q^2)}{M_B}\right)\,\bar{\ell}(p_2)\gamma_\mu\gamma_5\ell(-p_1)\right]. \end{aligned} \tag{2.4}$$

---

[2] Our notations and conventions are: $\gamma^5 = i\gamma^0\gamma^1\gamma^2\gamma^3$, $\sigma_{\mu\nu} = \frac{i}{2}[\gamma_\mu,\gamma_\nu]$, $\varepsilon^{0123} = -1$, $\epsilon_{abcd} \equiv \epsilon_{\alpha\beta\mu\nu}a^\alpha b^\beta c^\mu d^\nu$, $e = \sqrt{4\pi\alpha_{\rm em}}$.

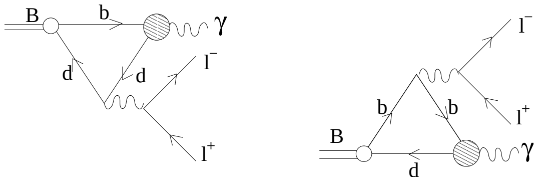

Fig. 2: Diagrams contributing to $B_d \to \ell^+\ell^-\gamma$ discussed in section II B. Dashed circles denote the $b \to d\gamma$ operator $O_{7\gamma}$.

B. Direct emission of the virtual photon from valence quarks of the B meson

This process is described by diagrams of Fig. 2: the real photon is emitted from the penguin, whereas one of the valence quarks directly emits the virtual photon which then goes into the final $\ell^+\ell^-$ pair. The corresponding amplitude $A^{(2)}_\mu$ has the same structure as the $C_{7\gamma}$ part of the amplitude $A^{(1)}_\mu$ with $F_{TA,TV}(q^2,0)$ replaced by $F_{TA,TV}(0,q^2)$. The form factors $F_{TA,TV}(0,q^2)$ at the necessary timelike momentum transfers are not known. The difficulty with these form factors comes from neutral light vector mesons, ρ^0 and ω for B_d decay and ϕ for B_s decay, which appear in the physical $B \to \gamma\ell^+\ell^-$ decay region. These resonances emerge in the amplitude of the subprocess when the photon is emitted from the light valence d or s quark. We obtain the form factors $F_{TA,TV}(0,q^2)$ for $q^2 > 0$ using gauge-invariant version [12] of the vector meson dominance [13]. This allows us to express the form factors $F_{TA,TV}(0,q^2)$ in terms of the $B \to V$ transition form factors at zero momentum transfer and leptonic constants of vector mesons

$$F_{TV,TA}(0,q^2) \;=\; F_{TV,TA}(0,0) \;-\; \sum_V 2\, f_V g_+^{B\to V}(0)\frac{q^2/M_V}{q^2 \;-\; M_V^2 \;+\; iM_V\Gamma_V}, \tag{2.5}$$

M_V and Γ_V being the mass and width of the vector meson resonance. The $B \to V$ transition form factors are defined according to relations

$$\langle V(q,\varepsilon)|\bar d\sigma_{\mu\nu}b|B(p)\rangle \;=\; i\varepsilon^{*\alpha}\,\epsilon_{\mu\nu\beta\gamma}\left[g_+^{B\to V}(k^2)g_{\alpha\beta}(p+q)^\gamma + g_-^{B\to V}(k^2)g_{\alpha\beta}k^\gamma + g_0^{B\to V}(k^2)p_\alpha p^\beta q^\gamma\right]. \tag{2.6}$$

The leptonic decay constant of a vector meson is given by

$$\langle 0|\bar d\gamma_\mu d|V(\varepsilon,p)\rangle = \varepsilon_\mu M_V f_V. \tag{2.7}$$

We shall use the form factors $g^{B\to V}$ calculated in [14] using the relativistic dispersion approach [15].

Notice that the resonance contribution discussed in this Section is similar to the resonance contribution in the Wilson coefficient $C_{9V}^{\rm eff}$ which emerge due to 4-quark operators. In the case of $C_{9V}^{\rm eff}$ vector mesons containing $\bar cc$ and $\bar uu$ pairs contribute.

C. Weak annihilation

The weak annihilation amplitude $A^{\rm WA}$ is given by triangle diagrams of Fig 3. One should take into account u and c quarks in the loop. The vertex describing the $\bar bd \to \bar UU$ transition ($U = u, c$) reads

$$H_{\rm eff}^{B\to\bar UU} = -\frac{G_F}{\sqrt2}\,a_1\,V_{Ub}V_{Ud}^*\,\bar d\gamma_\mu(1-\gamma_5)b\,\bar U\gamma_\mu(1-\gamma_5)U, \tag{2.8}$$

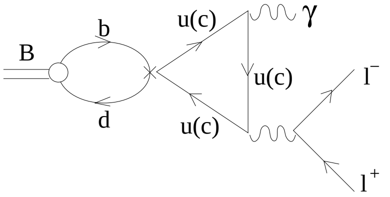

Fig. 3: Weak annihilation diagrams discussed in section II C. Triangle diagrams with u and c quarks in the loop should be taken into account.

with $a_1 = C_1 + C_2/N_c$, N_c number of colors [16]. For $N_c = 3$ one finds $a_1 = -0.13$. We now have to take

$$\langle \ell^+ \ell^- \gamma | H_{\rm eff}^{B\to \bar U U} | B \rangle. \tag{2.9}$$

The $\bar U U$ contribution to this amplitude can be written as

$$A_\mu^{WA}(\bar U U) = \frac{G_F}{\sqrt{2}} V_{Ub} V_{Ud}^* a_1 2 e^3 \epsilon_{\mu \varepsilon^* q k} \frac{G_{\gamma\gamma}(M_B^2, k^2 = 0, q^2 | m_U^2)}{q^2}\, \bar\ell^+ \gamma_\mu \ell^-, \tag{2.10}$$

where the form factor $G(p^2, k^2, q^2 | m_U^2)$ is defined as follows [17]

$$\langle \gamma^*(k) \gamma^*(q) | \partial^\nu (\bar U \gamma_\nu \gamma_5 U) | 0 \rangle = e^2 \varepsilon^{*\alpha}(k) \varepsilon^{*\beta}(q) \epsilon_{\alpha\beta k q} G_{\gamma\gamma}(k^2, q^2, p^2 | m_U^2). \tag{2.11}$$

For massless u-quark in the loop, axial anomaly [18] fixes the form factor $G_{\gamma\gamma}(p^2, k^2, q^2|0) = -\frac{2N_c(Q_U)^2}{4\pi^2}$. For c-quark there is additional q^2-dependent contribution given by the amplitude $m_c \langle \gamma^*(k)\gamma^*(q) | \bar c \gamma_5 c) | 0 \rangle \sim m_c^2/M_B^2$, which contains ψ and ψ' resonances at $q^2 > 0$. The latter contribution is numerically negligible compared to contributions discussed in the previous sections for all q^2 in the reaction of interest. Therefore, we have

$$A_\mu^{WA} = -\frac{G_F}{\sqrt{2}} \alpha_{\rm em} e\, a_1 \{ V_{ub} V_{ud}^* + V_{cb} V_{cd}^* \} \frac{16}{3} \epsilon_{\mu \varepsilon^* q k} \frac{1}{q^2}\, \bar\ell^+ \gamma_\mu \ell^-. \tag{2.12}$$

The anomalous contribution is enhanced at small q^2, but even here it is suppressed by a power of a heavy quark mass compared to the contributions discussed in the previous sections [11, 19].

D. Bremsstrahlung

Fig. 4 gives diagrams describing Bremsstrahlung. The corresponding contribution to the $B \to \ell^+ \ell^- \gamma$ amplitude reads

$$A_\mu^{\rm Brems} = i\, e \frac{G_F}{\sqrt{2}} \frac{\alpha_{\rm em}}{2\pi} V_{td}^* V_{tb} \frac{f_{B_q}}{M_B} 2 \hat m_\ell\, C_{10A}(\mu)\, \bar\ell(p_2) \left[\frac{(\gamma\epsilon^*)\,(\gamma p)}{\hat t - \hat m_\ell^2} - \frac{(\gamma p)\,(\gamma \epsilon^*)}{\hat u - \hat m_\ell^2} \right] \gamma_5\, \ell(-p_1). \tag{2.13}$$

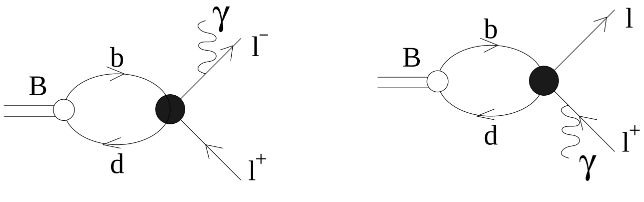

Fig. 4: Diagrams describing photon Bremsstrahlung. Solid circles denote the operator O_{10A}.

III. THE $B \to \ell^+ \ell^- \gamma$ CROSS-SECTION

The amplitudes discussed in Sections II A-II C have the same Lorentz structure, whereas the structure of the Bremsstrahlung amplitude (Section II D) is different. Therefore, it is convenient to write the cross-section as the sum of three contributions: square of the amplitude A^{1+2+WA} which we denote $\Gamma^{(1)}$, square of the amplitude $A^{\rm Brems}$ which we denote $\Gamma^{(2)}$, and their mixing, denoted as $\Gamma^{(12)}$:

$$
\begin{aligned}
\frac{d^2\Gamma^{(1)}}{d\hat{s}\, d\hat{t}} &= \frac{G_F^2\, \alpha_{em}^3\, M_1^5}{2^{10}\, \pi^4} \left| V_{tb}\, V_{tq}^* \right|^2 \Big[x^2\, B_0\left(\hat{s},\, \hat{t}\right) \,+\, x\, \xi\left(\hat{s}, \hat{t}\right)\, \tilde{B}_1\left(\hat{s},\, \hat{t}\right) \,+\, \xi^2\left(\hat{s}, \hat{t}\right)\, \tilde{B}_2\left(\hat{s},\, \hat{t}\right) \Big], \qquad (3.1)\\
B_0\left(\hat{s},\, \hat{t}\right) &= \left(\hat{s} \,+\, 4\hat{m}_\ell^2\right) \left(F_1\left(\hat{s}\right) \,+\, F_2\left(\hat{s}\right)\right) \,-\, 8\hat{m}_\ell^2\, \left|C_{10A}(\mu)\right|^2 \left(F_V^2\left(q^2\right) \,+\, F_A^2\left(q^2\right)\right),\\
\tilde{B}_1\left(\hat{s},\, \hat{t}\right) &= 8\, \Big[\hat{s}\, F_V(q^2)\, F_A(q^2)\, Re\left(C_{9V}^{eff\,*}(\mu, q^2)\, C_{10A}(\mu)\right)\\
&\quad + \hat{m}_b\, F_V(q^2)\, Re\left(C_{7\gamma}^*(\mu)\, \bar{F}_{TA}^*(q^2)\, C_{10A}(\mu)\right) + \hat{m}_b\, F_A(q^2)\, Re\left(C_{7\gamma}^*(\mu)\, \bar{F}_{TV}^*(q^2)\, C_{10A}(\mu)\right) \Big],\\
\tilde{B}_2\left(\hat{s},\, \hat{t}\right) &= \hat{s}\, \left(F_1\left(\hat{s}\right) \,+\, F_2\left(\hat{s}\right)\right),\\
F_1\left(\hat{s}\right) &= \left(\left| C_{9V}^{\rm eff}(\mu, q^2) \right|^2 \,+\, \left|C_{10A}(\mu)\right|^2 \right) F_V^2(q^2) \,+\, \left(\frac{2\hat{m}_b}{\hat{s}}\right)^2 \left| C_{7\gamma}(\mu)\, \bar{F}_{TV}(q^2) \right|^2\\
&\quad + \frac{4\hat{m}_b}{\hat{s}}\, F_V(q^2)\, Re\left(C_{7\gamma}(\mu)\, \bar{F}_{TV}(q^2)\, C_{9V}^{eff\,*}(\mu, q^2)\right),\\
F_2\left(\hat{s}\right) &= \left(\left| C_{9V}^{\rm eff}(q^2, \mu) \right|^2 \,+\, \left|C_{10A}(\mu)\right|^2 \right) F_A^2(q^2) \,+\, \left(\frac{2\hat{m}_b}{\hat{s}}\right)^2 \left| C_{7\gamma}(\mu)\, \bar{F}_{TA}(q^2) \right|^2\\
&\quad + \frac{4\hat{m}_b}{\hat{s}}\, F_A(q^2)\, Re\left(C_{7\gamma}(\mu)\, \bar{F}_{TA}(q^2)\, C_{9V}^{eff\,*}(\mu, q^2)\right).
\end{aligned}
$$

$$
\frac{d^2\Gamma^{(2)}}{d\hat{s}\, d\hat{t}} = \frac{G_F^2\, \alpha_{em}^3\, M_1^5}{2^{10}\, \pi^4} \left| V_{tb}\, V_{tq}^* \right|^2 \left(\frac{8\, f_{B_q}}{M_B}\right)^2 \hat{m}_\ell^2\, \left|C_{10A}(\mu)\right|^2 \left[\frac{\hat{s} \,+\, x^2/2}{(\hat{u} \,-\, \hat{m}_\ell^2)(\hat{t} \,-\, \hat{m}_\ell^2)} \,-\, \left(\frac{x\, \hat{m}_\ell}{(\hat{u} \,-\, \hat{m}_\ell^2)\,(\hat{t} \,-\, \hat{m}_\ell^2)} \right)^2 \right] \qquad (3.2)
$$

$$
\begin{aligned}
\frac{d^2\Gamma^{(12)}}{d\hat{s}\, d\hat{t}} &= \frac{G_F^2\, \alpha_{em}^3\, M_1^5}{2^{10}\, \pi^4} \left| V_{tb}\, V_{tq}^* \right|^2 \frac{16\, f_{B_q}}{M_B}\, \hat{m}_\ell^2\, \frac{x^2}{(\hat{u} \,-\, \hat{m}_\ell^2)(\hat{t} \,-\, \hat{m}_\ell^2)} \qquad (3.3)\\
&\times \left[\frac{2\, x\, \hat{m}_b}{\hat{s}}\, Re\left(C_{10A}^*(\mu) C_{7\gamma}(\mu) \bar{F}_{TV}(q^2, 0)\right) \,+\, x\, F_V(q^2)\, Re\left(C_{10A}^*(\mu) C_{9V}^{\rm eff}(\mu, q^2)\right) \,+\, \xi(\hat{s}, \hat{t})\, F_A(q^2)\, \left|C_{10A}(\mu)\right|^2 \right].
\end{aligned}
$$

Here

$$
\hat{s} \,=\, \frac{(p \,-\, k)^2}{M_B^2}, \qquad \hat{t} \,=\, \frac{(p \,-\, p_1)^2}{M_B^2}, \qquad \hat{u} \,=\, \frac{(p \,-\, p_2)^2}{M_B^2}. \qquad (3.4)
$$

with $\hat{s} \,+\, \hat{t} \,+\, \hat{u} \,=\, 1 \,+\, 2\hat{m}_\ell^2$, $\hat{m}_\ell^2 \,=\, m_\ell^2/M_B^2$, $\hat{m}_b \,=\, m_b/M_B$ and [4]

$$
x \,=\, 1 \,-\, \hat{s}, \qquad \cos\theta \,=\, \frac{\xi\left(\hat{s}, \hat{t}\right)}{x\, \sqrt{1 \,-\, 4\hat{m}_l^2/\hat{s}}}, \qquad \xi\left(\hat{s}, \hat{t}\right) \,=\, \hat{u} \,-\, \hat{t}. \qquad (3.5)
$$

In the above formulas the complex form factors $\bar{F}_{TV,TA}$ and defines as follows

$$
\begin{aligned}
\bar{F}_{TV}(q^2) &= F_{TV}(q^2, 0) + F_{TV}(0, q^2) - \frac{16}{3} \frac{V_{ub} V_{ud}^* + V_{cb} V_{cd}^*}{V_{tb} V_{td}^*} \frac{a_1}{C_{7\gamma}} \frac{f_B}{m_b},\\
\bar{F}_{TA}(q^2) &= F_{TA}(q^2, 0) + F_{TA}(0, q^2). \qquad (3.6)
\end{aligned}
$$

The expressions (3.2) and (3.3) contain the infrared pole which requires a cut in the energy of the emitted photon. Clearly, the contribution of the pole is proportional to the lepton mass.

IV. NUMERICAL ANALYSIS

A. Parameters

For numerical estimates we use the following values:

- The Wilson coefficients at $\mu = 5$ GeV corresponding to $C_2(M_W) = -1$:
  $C_1(5\,GeV) = 0.241$, $C_2(5\,GeV) = -1.1$, $C_{7\gamma}(5\,GeV) = 0.312$, $C_{9V}(5\,GeV) = -4.21$, $C_{10A}(5\,GeV) = 4.64$ [3].
- The CKM matrix elements $|V_{tb}^* V_{td}| = (8.3 \pm 1.6)10^{-3}$, $|V_{tb}^* V_{ts}| = (4.7 \pm 0.8)10^{-2}$ [20].
- The B-meson lifetimes $\tau(B_d) = 1.536 \pm 0.014$ ps and $\tau(B_s) = 1.461 \pm 0.057$ ps [20].
- For the $B_d \to \gamma$ form factors we use parametrizations from [4]

$$F_i(q^2) \;=\; \beta_i \frac{f_B M_B}{\Delta_i + E^\gamma}, \qquad E^\gamma = \frac{M_B}{2}\left(1 - \frac{q^2}{M_B^2}\right), \tag{4.1}$$

  with $i = V, A, TV, TA$ and the parameters β and Δ given in Table 1.

Table 1: Parameters for the form factors in Eq. (4.1) from [4]

Parameter	F_V	F_{TV}	F_A	F_{TA}
β (GeV^{-1})	0.28	0.30	0.26	0.33
Δ (GeV)	0.04	0.04	0.30	0.30

- The form factors $g_+^{B\to V}$ at $q^2 = 0$ for $B_d \to \rho^0$, $B_d \to \omega$ transitions and $B_s \to \phi$ are given in Table 2. The $B_s \to \gamma$ and the $B_d \to \gamma$ form factors are taken to be equal to each other.

Table 2: The leptonic decay constants f_V and the $B \to V$ transition form factors $g_+^{B\to V}$ at $q^2 = 0$.

	ρ^0	ω	ϕ
f_V (MeV)	154	45.3	-58.8
$g_+^{B^0\to V}(0)$	0.19	$-\,0.19$	$-\,0.38$

B. Results

The calculated dilepton differential distributions are shown in Fig. 5 for different leptons in the final state and for different values of the photon energy cut - the minimal photon energy in the B-meson rest frame E^γ_{min}. Table 3 gives the dependence of the integrated $B_{d,s} \to \ell^+\ell^-\gamma$ decay rate on E^γ_{min}. A particular choice of E^γ_{min} depends on the energy resolution in a specific experiment: namely, $E^\gamma_{min} = 80$ MeV and $E^\gamma_{min} = 20$ MeV in Table 3 correspond to the expected accuracy of the B-meson reconstruction of ATLAS and LHCb, respectively.

Table 3: The $B_{d,s} \to \ell^+\ell^-\gamma$ decay rates as functions of the minimal photon energy E^γ_{min}. The region of the J/ψ and ψ' resonances $0.33 \le \hat{s} \le 0.55$ was excluded from the $\hat{s}$ integration, that corresponds to the experimental procedure adopted at LHC [2, 21].

m_ℓ	m_e			m_μ			m_τ		
E^γ_{min} (MeV)	20	50	80	20	50	80	20	50	80
$Br\left(B_d \to \ell^+\ell^-\gamma\right) \times 10^{10}$ [This work]	3.95	3.95	3.95	1.34	1.32	1.31	3,39	2.37	1.87
$Br\left(B_s \to \ell^+\ell^-\gamma\right) \times 10^{9}$ [This work]	24.6	24.6	24.6	18,9	18.8	18.8	11.6	8.10	6.42
$Br\left(B_d \to \ell^+\ell^-\gamma\right) \times 10^{10}$ [5]	1.01	1.01	1.01	0.66	0.62	0.61	3.39	2.38	1.88
$Br\left(B_s \to \ell^+\ell^-\gamma\right) \times 10^{9}$ [5]	3.30	3.29	3.29	2.16	2.06	2.00	11.6	8.15	6.47
$Br\left(B_s \to \ell^+\ell^-\gamma\right) \times 10^{9}$ [6]	20	20	20	12	12	12	–	–	–

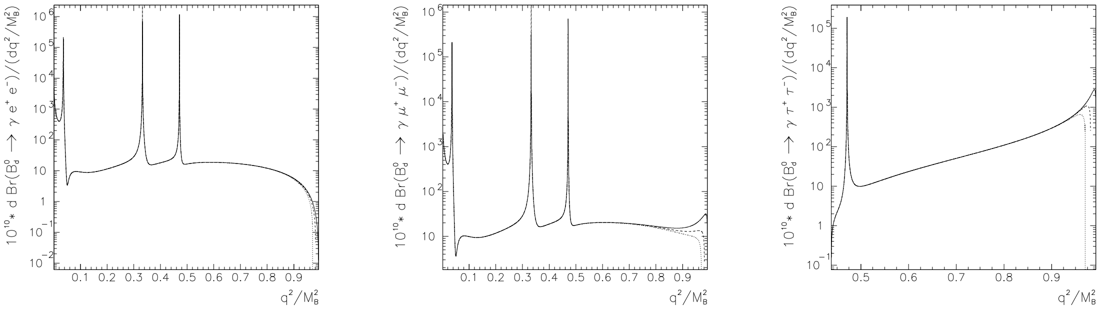

Fig. 5: Dilepton q^2-spectrum in $B_s \to e^+e^-\gamma$ (left), $B_s \to \mu^+\mu^-\gamma$ (central), and $B_s \to \tau^+\tau^-\gamma$ (right) for different photon energy cuts: $E^{\gamma}_{min} = 20$ MeV (solid), $E^{\gamma}_{min} = 50$ MeV (dashed), $E^{\gamma}_{min} = 80$ MeV (dotted).

Our results for the *integrated* decay rate in Table 3 are close to the results reported in [6]. Notice however that in [6] resonance contributions were not considered and the $B \to \gamma$ form factors corresponding to the limit $m_b \to \infty$ were used. As shown in [4], corrections to the asymptotic formulas in $B \to \gamma$ form factors at large q^2 are rather large, therefore the *differential* distributions calculated here differ strongly from those of [6].[3] Our results both for the integrated and the differential distributions in the $B \to e^+e^-\gamma$ and $B \to \mu^+\mu^-\gamma$ decays in the region $q^2 \lesssim 2$ GeV differ strongly from the results of [5] where the contribution of the direct virtual photon emission from valence quarks of the B-meson (Section II B) was not taken into account (Figs. 6, 7).

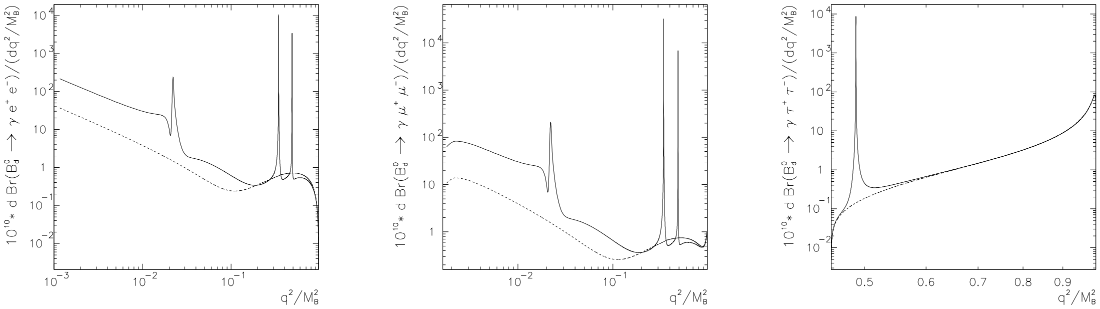

Fig. 6: Dilepton q^2-spectrum in B_d decays: $B_d \to e^+e^-\gamma$ (left), $B_d \to \mu^+\mu^-\gamma$ (central), and $B_d \to \tau^+\tau^-\gamma$ (right) for $E^{\gamma}_{min} = 20$ MeV. Solid line - our result; dashed line - result corresponding to [5], where the contribution of the direct virtual photon emission from valence quarks of the B meson (Section II B) was not taken into account.

V. CONCLUSIONS

We studied the $B_{d,s} \to \ell^+\ell^-\gamma$ decays taking into account photon emission from the b-quark loop, weak annihilation, and Bremsstrahlung from leptons in the final state. Special emphasis was laid on long-distance QCD effects in $B \to \ell^+\ell^-\gamma$ decays related to the photon emission from the b-quark loop. The contribution of light vector-meson

---

[3] Let us point out that in distinction to the J/ψ and ψ', the region of light vector resonances will not be excluded from the experimental analysis. That is because for small values of $\hat{s}$ photons have sufficient energies to be registered in the electromagnetic calorimeter. Moreover, the region of small $\hat{s}$ gives the main contribution to the $B \to \mu^+\mu^-\gamma$ signal at LHC. For $B_s \to e^+e^-\gamma$ and $B_s \to \mu^+\mu^-\gamma$ decays, the ϕ-meson resonance contribution leads to a strong enhancement of the full spectrum compared to the non-resonance one.

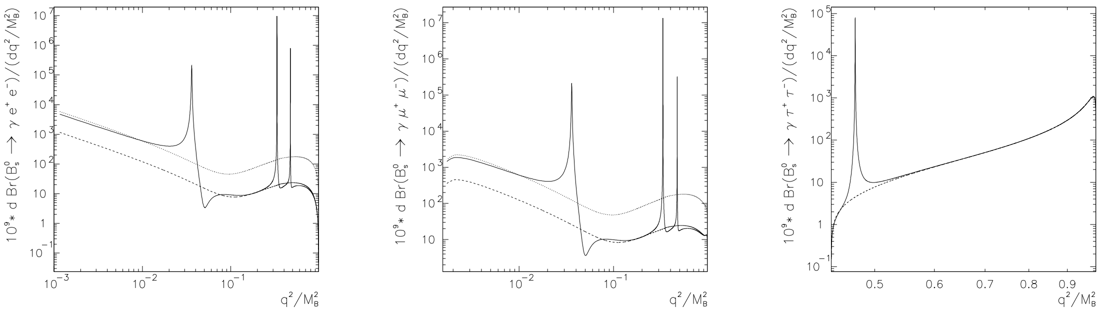

Fig. 7: Dilepton q^2-spectrum in B_s decays: $B_s \to e^+e^-\gamma$ (left), $B_s \to \mu^+\mu^-\gamma$ (central), and $B_s \to \tau^+\tau^-\gamma$ (right) for $E^{\gamma}_{min} = 20$ MeV. Solid line - our result, dashed line - [5], dotted line - [6].

resonances related to the direct virtual photon emission from valence quarks of the B-meson, not taken into account in previous analyses, was shown to be essential for a proper description of the process. In particular, this contribution affects stongly dilepton mass spectra in processes with light leptons in the final state. Reliable predictions for dilepton mass spectrum in $B_{d,s} \to \ell^+\ell^-\gamma$ decays within the Standard Model were given.

Acknowledgments

We would like to thank L.Sehgal for clarifications concerning his work and L.Smirnova for stimulating discussions. We gratefully acknowledge financial support under a Rückkehr Stipendium of the Alexander von Humboldt-Stiftung (D.M.) and the INTAS grant YSF2001/2-122 (N.N.).

---

[1] A.Ali, hep-ph/9606324; M.Battaglia et al, *The CKM matrix and the unitarity triangle*, hep-ph/0304132.
[2] P.Ball et. al., B Decays, in *Proceedings of the Workshop on Standard Model Physics (and more) at the LHC*, CERN 2000-004 (2000).
[3] B.Grinstein, M.Wise and M.Savage, Nucl.Phys. B**319**, 271 (1989); A.J.Buras and M.Munz, Phys.Rev. D**52**, 186 (1995).
[4] F.Kruger and D.Melikhov, Phys.Rev. D**67**, 034002 (2003).
[5] C.Q.Geng, C.C.Lih, W.M.Zhang, Phys.Rev. D**62**, 074017 (2000).
[6] Yu.Dincer and L.M.Sehgal, Phys.Lett. B**521**, 7 (2001).
[7] S.Descotes-Genon, C.T.Sachrajda, Phys.Lett. B**557**, 213 (2003).
[8] T.M.Aliev, A.Ozpineci, M.Savci, Phys.Rev. D**55**, 7059 (1997).
[9] F.Kruger and L.M.Sehgal, Phys.Rev. D**55**, 2799 (1997); D.Melikhov, N.Nikitin, S.Simula, Phys.Lett. B**430**, 332 (1998); Phys.Rev. D**57**, 6814 (1998).
[10] G.P.Korchemsky, D.Pirjol, T.-M.Yan, Phys.Rev. D**61**, 114510 (2000).
[11] S.Bosch and G.Buchalla, JHEP **0208**, 054 (2002).
[12] D.Melikhov, Phys.Lett. B**516**, 61 (2001), D.Melikhov, O.Nachtmann, V.Nikonov, T.Paulus, Eur.Phys.J. C**34**, 345 (2004).
[13] J.J.Sakurai, Ann.Phys. **11**, 1 (1960); M.Gell-Mann, F.Zachariasen, Phys.Rev. **124**, 953 (1961); G.J.Gounaris, J.J.Sakurai, Phys.Rev.Lett. **21**, 244 (1968).
[14] D.Melikhov, B.Stech, Phys.Rev. D**62**, 014006 (2000).
[15] D.Melikhov, Phys.Rev. D**53**, 2460 (1996); Phys.Rev. D**56**, 7089 (1997).
[16] M.Neubert, B.Stech, hep-ph/9705292.
[17] D.Melikhov, B.Stech, Phys.Rev.Lett. **88**, 151601 (2002).
[18] S.Adler, Phys.Rev. **177**, 2426 (1969); J.Bell and R.Jackiw, Nuovo Cimento 60**A**, 47 (1969).
[19] M.Beyer, D.Melikhov, N.Nikitin, B.Stech, Phys.Rev. D**64**, 094006 (2001).
[20] S.Eidelmen et al, Phys.Lett. B**592**, 1 (2004).
[21] N.Nikitin et al, Yad.Fiz. **62**, 1823 (1999).